Applications and new developments in Resistive Plate Chambers

P. Fonte

Abstract-- Resistive Plate Chambers are rugged and affordable gas detectors that have found extensive use in High Energy Physics and Astroparticle experiments. The main features of these counters are the very large pulse height, reduced cost per unit area and good (about 1 ns) time resolution.

The field has enjoyed very lively progress in recent years, including the introduction of a new (avalanche) mode of operation, extension of the counting rate capabilities to levels around 10 MHz/cm^2, improvement of the time resolution for MIPs to 50 ps s and the achievement of position resolutions of a few tens of μm.

These new developments have extended the range of HEP applications and promise new applications in medical imaging.

I. Introduction

Resistive Plate Counters (RPCs) were introduced in 1981 [1] as a practical alternative to the remarkable "Localized discharge spark counters" [2], which ultimately achieved a time resolution of 25 ps s [3]. The resulting detector, being by construction free from damaging discharges and enjoying a time resolution of the order of 1 ns, has found very good acceptance in High Energy and Astroparticle Physics.

In modern language the original RPCs were single-gap counters operated in streamer mode. Soon the double-gap structure was introduced [4] to improve the detection efficiency along with the avalanche mode of operation [5], which extends its counting rate capabilities.

An imaginative construction method, denominated "multigap RPC" was introduced in 1996 [6], being specially suited for the construction of counters with more than a single gas gap.

Recent innovations in detector construction and readout electronics have extended the timing resolution of RPCs for minimum ionizing particles (MIPs) to 50 ps s [7], the rate capability to 10^5 Hz/mm^2 [8] and the position resolution for X-rays to 30 μm FWHM in digital readout mode [9].

Single and double-gap streamer-mode RPCs have so far found application in cosmic ray experiments, like COVER_PLASTEX [10] and EAS-TOP [11] being also used in the High Energy Physics experiments L3 at CERN, BABAR at SLAC, USA and BELLE at KEK, Japan. Future applications will include the ARGO experiment at the "YangBaJing High-altitude Cosmic Ray Laboratory" [12] and the OPERA [13] and MONOLITH [14] cosmic ray experiments in LNGS, Italy. The Muon Arm of the ALICE experiment at LHC [15] will also be equipped with streamer-mode RPCs.

Avalanche-mode RPCs will be used for the muon trigger systems of the ATLAS [16], CMS [17] and LHCb [18] experiments at LHC.

Timing RPCs, a recent development [19], are already in use by the HARP experiment at the CERN PS accelerator [20] and will equip the 160 m^2 TOF barrel of ALICE's Particle Identification Detector [21].

II. RPC designs

The combination of resistive and metallic electrodes with signal-transparent semi-conductive layers, highly isolating layers and different kinds of pickup electrodes endows the RPCs with a rich variety of configurations, tunable to a variety of requirements.

A. Single gap

The original RPC design [1], included a single gas gap delimited by bakelite resistive electrodes. Naturally the counter design has evolved since then and a modern example is shown in Fig. 1.

The application of the polarizing potential to the resistive electrode via an electrode with a lower resistivity, but still transparent to the induced signals (see for instance [22], [23]) allows to operate both signal pickup electrodes at ground potential, saving the utilization of high-voltage capacitors and avoiding the need for high voltage insulation of the strips.

Glass electrodes, enjoying a mechanical stiffness and surface quality much superior to bakelite, have also been considered in the past and remain in use today (eg. [2], [24], [25]).

B. Double gap

Double-gap designs [4], having a larger number of elements (gas gaps, pickup electrodes), allow for more varied structures than the single gap ones and two such designs are presented as examples in Fig. 2.

C. "Multigap"

A construction method denominated "multigap RPC" was introduced in 1996 [6], being especially well suited for the

Manuscript received November 25, 2001. This work was supported by Fundação para a Ciência e Tecnologia in the framework of the project CERN/P/FIS/40111/2000.

P. Fonte is with ISEC and LIP, Coimbra University, Coimbra P-3000, Portugal (e-mail: .fonte@lipc.fis.uc.pt).

construction of counters with more than a single gas gap. A schematic drawing is shown in Fig. 3.
The most preeminent feature of this design is the inclusion of resistive, electrically floating, electrodes that divide the gas volume into a number of individual gas gaps, without the need of any conductive electrodes. According to its inventors the steady-state requirement for a null total current on each of the dividing electrodes stabilizes their potential at a value that equalizes the currents flowing in and out by adjusting the gas gain in the neighboring gaps.
Possible drawbacks of this design are the large voltages required and the fact that at low ionizing particle fluxes the stabilizing mechanism may be dominated by the dark counting rate.

D. Hybrid designs

Metallic and resistive electrodes may be combined and still retain the main property of the RPC: the total absence of violent discharges. The only requirement is that no gas gap will be delimited by two metallic electrodes.
Actually the gas counter formed by two parallel metallic electrodes defining a gas gap is denominated Parallel Plate Chamber (PPC), which has found wide application in the detection of heavy ions and, with wire-mesh electrodes, proposed long ago for high-rate applications [26]. However, possibly due to the violent nature of the discharges, this type of counter never found wide acceptance in HEP.
A few schematic examples of hybrid RPCs can be seen in Fig. 4.

III. Modes of Operation

A. Nature of the operation modes

RPCs may be operated in avalanche mode or discharge mode.
The avalanche mode corresponds to the generation in the gas gap of a Townsend avalanche, following the release of primary charge by the incoming ionizing radiation.
In discharge mode the avalanche is followed by a "streamer" discharge [27]. In a metallic counter the discharge will evolve via a sequence stages comprising avalanche, streamer, glow discharge, filamentary discharge and spark [28]. However the later discharge stages require a considerable current, up to few Amperes, to flow in the gap, which is forbidden by the high resistivity of the RPC electrodes.
Optical observations suggest that in glass RPCs the discharge is quenched at the filamentary discharge stage ([29], [30]). However, for electrode resistivities of the order of $4\times10^{7}\ \Omega\,\mathrm{cm}$, a permanent glow discharge could sometimes be observed [8].

B. Space charge effect

The space charge present in a Townsend avalanche creates its own electric field that is summed to the applied electric field. Three regions can be identified: the total field is larger than the applied field immediately upstream and downstream from the avalanche and lower than the applied field over the main avalanche body [31]. For avalanches approaching 10^{8} electrons (the Raether limit [27]), the high-field regions generate the conditions for the development of the cathode and anode (backward and forward) streamers, while the lower field region causes the reduction of gas gain seen by the avalanche (avalanche saturation effect) [27]. Both phenomena, avalanche saturation and streamers, share a common physical origin and are normally simultaneously present.
The existence of a strong avalanche saturation effect in RPCs has been experimentally verified and has been shown to play a central role in the interpretation of the charge spectra and efficiency characteristics, both for millimetric ([32], [33]) and sub-millimetric ([34], [35]) gas gaps.

C. Available signal

The charge signal ranges from a few pC for the fast (electron) component of the signal in avalanche mode to a range between 50 pC [36] and a few nC ([37] for instance) in streamer mode.
Naturally, due to the high resistivity of the electrodes, there is a tradeoff between the available signal charge and the counting rate capability (see section V).

D. Gas mixtures

Modern standard RPCs working in avalanche mode use mostly mixtures of tetrafluoroethane ($C_2H_2F_4$) with 2 to 5% of isobutane (iso-C_4H_{10}) and 0.4% to 10% of sulphur hexafluoride (SF_6). The addition of SF_6 has been shown to extend the streamer-free operation region and to reduce the amount of charge in the streamer ([32], [38]).
In streamer mode mixtures of argon with isobutane and tetrafluoroethane in widely varying proportions tend to be used.
It was recently shown the addition of SF_6 (4%) to the remaining constituents allowed to reduce the streamer charge to 50 pC and extend the counting rate capability to 300 Hz/cm^2, while keeping efficient streamer-mode operation [36].

IV. Efficiency for MIPs

In Fig. 5 a survey of recently published results concerning the efficiency of RPCs for MIPs is shown. For the sake of comparison the reported efficiency of multiple-gap chambers was converted to an efficiency per gap ($e_{(1\,gap)}$) figure by using the formula

$$e_{(1\,gap)} = 1-\bar{e}_{(1\,gap)} \approx 1-\sqrt[n]{(1-e_{(n\,gaps)})}\,, \qquad (1)$$

which considers the gas gaps as approximately independent counters.
It can be seen that most standard, 2 mm gap, RPCs show efficiencies per gap between 85% and 95%, irrespective of the operation mode. Smaller gap RPCs show a somewhat reduced efficiency, however it's still surprisingly large (45%)

for 0.1 mm gaps. The difficulties arising with the interpretation of such data have been addressed in [35].

V. Rate capability

A. Standard RPCs

In Fig. 6 a survey of recently published results concerning the counting rate capability of modern RPCs is presented as a function of the resistivity of the electrodes.

Only measurements taken with uniform and continuous illumination were considered. An over-optimistic estimation of the rate capabilities may arise if only a small area is irradiated (due to lateral currents in the electrodes) or if pulsed beams are used (see for instance [39]), presumably due to capacitive and electrode polarization effects. The maximum counting rate corresponds typically to a reduction in the counter efficiency by a few percent.

Present state-of–the-art standard high-rate RPCs reach 3 kHz/cm^2 in avalanche mode and 300 Hz/cm^2 in streamer mode. The data for the "multigap" RPC forms a different curve, seeming to offer an advantage in terms of counting rate capability for a given electrode resistivity.

B. Special RPCs

The combination of typical metallic counter structures like PPC or PPAC [26] with appropriated resistive electrodes yields discharge-tolerant counters that can reach very high counting rates.

In Fig. 7 the effective gas gain as a function of the counting rate is shown for some special RPCs. A PPAC with a low resistivity ($\tilde{n}=4\times10\hat{U}\,cm$) anode [8] and a microRPC (see also Fig. 4) with a Si cathode ($\tilde{n}=10^4\,\grave{U}\,cm$) and metallic anode ([40], [41]). Both devices reach the intrinsic counting rate limitation of metallic counters ([40], [42]), indicating that no further reduction of the electrode resistivity below $10\hat{U}\times cm$ is required for very high rate RPCs.

VI. Background counting rate

Due to the nature of the electrodes RPCs can accommodate relatively large background (dark) counting rates without much adverse effects. However such currents, above a limit, may affect the local and global rate capability, increase the occupancy of the readout electronics and induce faster ageing.

In TABLE I the published dark count rates of several counters are listed along with their mode of operation, the electrode material and the gap width. Is seems that 2 mm gap streamer-mode counters made of glass or bakelite often show dark counting rates on the order of 1 kHz/m^2. Thinner gap counters, like timing RPCs, show a larger dark counting rate, possibly on account of their much larger surface electric field.

These numbers should however be compared with the counting rate capabilities of standard RPCs reported in section V.A, ranging from 3×10^3 kHz/m^2 to 3×10^4 kHz/m^2.

The 0.4 mm counter made with very clean Si electrodes stands out as featuring a very high counting rate along with a low dark rate for such a small gap.

It should be noted that many authors quote the dark currents instead of the dark count rate. Since the dark currents include an unknown fraction of conduction current through the spacers and frames it is impossible to calculate which part corresponds to an effective counter occupancy.

The problem of understanding and reproducibly controlling the dark count rate of RPCs is one of the most important open problems for practical applications.

VII. Ageing

Although there is already some satisfactory long term operational experience in HEP experiments [43], where the irradiation dose is much larger than in cosmic ray physics, the difficulties encountered by the BABAR collaboration [44] will possibly motivate in the near future a revision of certain commonly accepted construction procedures.

VIII. Time resolution

A. Standard RPCs

A survey of recently published results concerning the time resolution of RPCs for MIPs as a function of the gap width is shown in Fig. 8.

Most standard, 2 mm gap, RPCs reach a resolution between 1 and 1.5 ns σ, independently of the operation mode. These results are normally taken using a simple leading-edge discrimination technique.

B. Timing RPCs

Timing RPCs have been recently developed [19] and reach currently a resolution of 50 to 60 ps s for electrode areas ranging from 9 cm^2 ([7], [45]) to 1600 cm^2 [46].

An array of 32 counters with an area of 9 cm^2 each (of the type described in [7]) has been also successfully tested, showing in particular a very small amount of crosstalk ([47], [48]).

The possibility of simultaneous bidimensional measurement of the avalanche position with millimetric accuracy and time measurement with a resolution of 50 ps s has been recently demonstrated in single-gap counters ([49], [50]) aimed to be applied in relatively small and very accurate TOF systems.

The principle of operation of timing RPCs is illustrated in Fig. 9, based on the model described in [35]. The initial current grows exponentially in time until the discriminating level is reached. The time delay is independent from the position occupied by the initial charges in the gap, providing excellent timing. The observed timing jitter dependents on the variation of the initial current (avalanche and cluster statistics) and inversely on the current growth rate $a\,v$, where a is the First Townsend Coefficient and v is the electron drift velocity. It is also clear from the figure that in

first approximation the timing accuracy should be independent of the discriminator level. Both this effect and the inverse dependence on $a\,v$ have been experimentally confirmed.

IX. Position Resolution

A. Standard RPCs

The majority of RPC applications do not require the determination of the avalanche position with accuracy better than ~1 cm and therefore little effort has been made to optimize their position resolution.

However a small study has been done with soft X-rays in an 8 mm gap RPC equipped with 0.38 mm pitch strips below the anodic resistive plate, yielding the position of the induced charge profile centroid with a resolution of 115 μm FWHM [51].

B. MicroRPC

A 100 μm gap RPC equipped with a solid X-ray converter and anodic strips placed at a pitch of 30 μm has shown a position resolution of at least 30 μm FWHM in digital counting mode [9].

A schematic view of the device is shown in Fig. 10, along with the most important results. The events could be mostly concentrated in a single 30 μm wide strip.

The reasons for this result are the good localization of the primary charge given by the solid converter and the fact that most of the charge in the avalanche (due to its exponential growth in space) is developed very close to anode, yielding a very narrow induced charge profile.

X. Conclusions and Outlook

Being robust (free of potentially damaging discharges) and affordable, standard RPCs enjoy today a wide acceptance in the HEP and Astroparticle community.

Two operation modes with similar efficiency and time resolution characteristics are available, with a tunable signal charge ranging from a few pC for the fast signal in avalanche mode to a range between 50 pC and a few nC in streamer mode.

The efficiency per gas gap for MIPs ranges from 45% for 0.1 mm gaps to 95% for the more common 2 mm gaps. Efficiencies above 99% are routinely reached by the use of 2 or more gaps sharing the same readout structure.

A good time resolution, from 1 to 2 ns σ, is also routinely achieved in either operation mode.

Present state-of-the-art counters reach counting rates up to a few kHz/cm^2 in avalanche mode and up to a few hundred Hz/cm^2 in streamer mode.

Recently some exciting developments have been made using special configurations.

Timing RPCs, made with glass electrodes that define several thin (0.2 to 0.3 mm) gas gaps, have reached a time resolution of 50 ps s , opening perspectives for affordable high-granularity TOF counters. This performance is kept at least up to an electrode area of 800 cm^2 per readout channel and seems to be independent of the number of gas gaps (at least up to 5).

Very high rate operation (10 MHz/cm^2 at a gain of 5×10^4) was demonstrated for two different counter constructions, both featuring medium resistivity electrodes (10^4 to$10\hat{U}\times$cm).

An excellent position resolution of 30 μm FWHM for X-rays in digital readout mode was also recently reported.

These new developments may open new applications in medical imaging and reliable high-rate tracking of MIPs [41].

XI. Acknowledgements

Special acknowledgements are due to Vladimir Peskov and Archana Sharma for their encouragement and support.

XII. References

[1] R. Santonico and R. Cardarelli, "Development of Resistive Plate Counters", *Nucl. Instr. Meth.*, vol. 187, pp. 377-380, 1981.

[2] V. V. Parkhomchuck, Yu. N. Pestov and N. V. Petrovykh, "A spark counter with large area", *Nucl. Instr. Meth.*, vol. 93, pp. 269-276, 1971.

[3] Yu. N. Pestov, Proc 5th Int. Conf. on Instrumentation for Colliding Beam Physics, Novosibirsk, pp. 163-165, 1984.

[4] R. Cardarelli and R. Santonico, A. di Biagio and A. Lucci, "Progress in resistive plate counters", *Nucl. Instr. Meth.*, vol. A263, pp. 20-25, 1988.

[5] R. Cardarelli, A. Di Ciaccio and R. Santonico, "Performance of a resistive plate chamber operating with pure CF3Br", *Nucl. Instr. Meth.*, vol. A333, pp. 399-403, 1993.

[6] E. Cerron Zeballos, I. Crotty, D. Hatzifotiadou, J. Lamas-Valverde, S. Neupane, M. C. S. Williams, A. Zichichi, "A new type of resistive plate chamber: the multigap RPC", *Nucl. Instr. Meth.*, vol. A374, pp. 132-135, 1996.

[7] P. Fonte, R. Ferreira-Marques, J. Pinhão, N. Carolino, A. Policarpo, "High-resolution RPCs for large TOF systems", *Nucl. Instr. Meth.*, vol. A449, pp. 295, 2000.

[8] P. Fonte, N. Carolino, L. Costa, Rui Ferreira-Marques, S. Mendiratta, V. Peskov, A. Policarpo, " A spark-protected high-rate detector", *Nucl. Instr. Meth.*, vol. A431, pp. 154-159, 1999.

[9] V. Peskov and P. Fonte, "Gain, Rate and Position Resolution Limits of Micropattern Gaseous Detectors", presented at the PSD99-5th International Conference on Position-Sensitive Detectors, London, England, 1999. Also preprint LIP/01-06 [Online]. Available: http://xxx.lanl. gov/abs/physics/0106017.

[10] M. Ambrosio, "Measurement of EAS thickness for individual events with RPCs in the GRES/COVER-PLASTEX experiment, *Scientifica Acta*, vol. 13, pp. 245-256, 1998.

[11] C. Aramo, "Arrival time measurement of muons in extensive air shower with bakelite RPC", *Scientifica Acta*, vol. 13, pp. 257-268, 1998.

[12] C. Bacci, K. Z. Bao, F. Barone, B. Bartoli, P. Bernardini, S. Bussino et al., "Results from the analysis of data collected with a 50 m RPC carpet at YangBaJing", *Nucl. Instr. Meth.*, vol. A456, pp. 121-125, 2000.

[13] S. Dusini, D. Autiero, E. Borsato, R. Brugnera, L. Camilleri, F. Dal Corso et al., "Design and prototype tests of the RPC system for the OPERA spectrometers", presented at the "RPC2001 – 6th Workshop on Resistive Plate Chambers and Related Detectors", 26-27th November 2001, Coimbra, Portugal.

[14] G. Bencivenni , C. Gustavino, H. Menghetti, F. Murtas, L. Satta, N. Redaelli, G. Trinchero, "Performance of a test prototype for MONOLITH", *Nucl. Instr. Meth.*, vol. A461, pp. 319-323, 2001.

[15] ALICE collaboration, "ALICE Muon Spectrometer technical design report", CERN, Geneva, report CERN/LHCC 99-22, 13 August 1999.

[16] ATLAS Muon collaboration, "ATLAS Muon Spectrometer Technical Design Report", CERN, Geneva, report CERN/LHCC 97-22, 5 June 1997.

[17] CMS Muon collaboration, "CMS muon technical design report", CERN, Geneva, report CERN/LHCC 97-32, 15 December 1997.

[18] LHCb Collaboration, CERN, Geneva, report "LHCb muon system technical design report", CERN-LHCC-2001-010, 28 May 2001.

[19] P. Fonte, A. Smirnitski and M. C. S. Williams, "A new high-resolution TOF technology", *Nucl. Instr. Meth.*, vol. A443, pp. 201-204, 2000.

[20] M. Bogomilov, D. Dedovich, R. Dumps, F. Dydak, V. Gapienko, A. Semak et al., "The RPC time-of-flight system of the HARP experiment", presented at "RPC2001 – 6th Workshop on Resistive Plate Chambers and Related Detectors", 26-27th November 2001, Coimbra, Portugal.

[21] ALICE collaboration, "ALICE TOF technical design report", CERN/LHCC 2000-012, Geneva : CERN, 16 February 2000.

[22] G. Battistoni, P. Campana, V. Chiarella, U. Denni, E. Iarocci and G. Nicoletti, "Resistive cathode transparency", *Nucl. Instr. Meth.*, vol. 202 pp. 459-464, 1982.

[23] H. Schöpf and B. Schnizer, "Theory describing cathode signals from charges moving in counters with a poorly conducting cathode", *Nucl. Instr. Meth.*, vol. A323, pp. 338-344, 1992.

[24] M. Anelli, G. Bencivenni, G. Felici and L. Macro, "Glass electrode spark counters", *Nucl. Instr. Meth.*, vol. A300, pp. 572-574, 1991.

[25] M. Yamaga, A. Abashian, K. Abe, K. Abe, P. K. Behera, S. Chidzik et al., "RPC systems for BELLE detector at KEKB", *Nucl. Instr. Meth.*, vol. A456, pp. 109-112, 2000.

[26] G. Charpak and F. Sauli, "The multistep avalanche chamber: a new high-rate high-accuracy gaseous detector", *Phys. Lett.*, vol. 78B, pp. 523-528, 1978.

[27] H. Raether, Electron Avalanches and Breakdown in Gases, London:Butterworths, 1964.

[28] S. C. Haydon, in Electrical Breakdown of Gases, ed. J. A. Rees, London: MacMillan, 1973, pp.146-172.

[29] I. Kitayama, H. Sakai, Y. Teramoto, S. Chinomi, Y. Inoue, E. Nakano, T. Takahashi, "Optical observation of discharge in resistive plate chamber", *Nucl. Instr. Meth.*, vol. A424, pp. 474-478, 1999.

[30] A. Semak, V. Ammosov, V. Gapienko, A. Ivanilov, V. Koreshev, A. Kulemzin, Yu. Sviridov, V. Zaets, E. Gushin and S. Somov, "Properties of discharge in the narrow gap glass RPC", *Nucl. Instr. Meth.*, vol. A456, pp. 50-54, 2000.

[31] P. Fonte, "A model of breakdown in parallel-plate detectors", *IEEE Trans. Nucl. Sci.*, vol. 43, pp. 2135-2146, 1996.

[32] P. Camarri, R. Cardarelli, A. Di Ciaccio, R. Santonico, "Streamer suppression with SF 6 in RPCs operated in avalanche mode", *Nucl. Instr. Meth.*, vol. A414, pp. 317-324, 1998.

[33] M. Abbrescia, A. Colaleo, G. Iaselli, F. Loddo, M. Maggi, B. Marangelli et al, "Progresses in the simulation of Resistive Plate Chambers in avalanche mode", *Nucl. Phys. B*, vol. 78, pp. 459-465, 1999.

[34] P. Fonte and V. Peskov, "High-Resolution TOF with RPCs", *Nucl. Instr. Meth.*, vol. A477, pp.17-22, 2002.

[35] P. Fonte, "High-Resolution Timing of MIPs with RPCs – a Model", *Nucl. Instr. Meth.*, vol. A456, pp. 6-11, 2000.

[36] R. Arnaldi, A. Baldit, V. Barret, N. Bastid, G. Blanchard, E. Chiavassa, et al., "Study of the resistive plate chambers for the ALICE Dimuon Arm", *Nucl. Instr. Meth.*, vol. A 456, pp. 73-76, 2000.

[37] C. Bacci, K. Z. Bao, F. Barone, B. Bartoli, P. Bernardini, R. Buonomo and the ARGO-YBJ Collaboration, "High altitude test of RPCs for the Argo YBJ experiment", *Nucl. Instr. Meth.*, vol. A443, pp. 342-345, 2000.

[38] V. Koreshev, V. Ammosov, A. Ivanilov, Yu. Sviridov, V. Zaets and A. Semak, "Operation of narrow gap RPC with tetrafluoroethane based mixtures", *Nucl. Instr. Meth.*, vol. A456, pp. 46-49, 2000.

[39] P. Colrain, G. Corti, L. de Paula, M. Gandelman, J. Lamas-Valverde, B. Marechal, D. Moraes, E. Polycarpo, B. Schmidt, T. Schneider and A. Wright, "Performance of a Multigap RPC prototype for the LHCb Muon system", *Nucl. Instr. Meth.*, vol. A456, pp. 62-66, 2000.

[40] C. Iacobaeus, M. Danielsson, P. Fonte, T. Francke, J. Ostling, V. Peskov, "Sporadic Electron Jets from Cathodes – The Main Breakdown-Triggering Mechanism in Gaseous Detectors", presented at the 2001 IEEE Nuclear Science Symposium, 4-10 November, San Diego, California, USA, 2001.

[41] T. Francke, P. Fonte, V. Peskov and J. Rantanen, "Potential of RPCs for tracking", presented at the RPC2001–6th Workshop on Resistive Plate Chambers and Related Detectors, 26-27th November 2001, Coimbra, Portugal.

[42] Y. Ivaniouchenkov, P. Fonte, V. Peskov, B. D. Ramsey, "Breakdown limit studies in high-rate gaseous detectors", *Nucl. Instr. Meth.*, vol. A422, pp. 300-304, 1999.

[43] A. Aloisio, M. G. Alviggi, S. Patricelli, C. Sciacca, G. Carlino, N. Cavallo, et al., "Long-term performance of the L3 RPC system", *Nucl. Instr. Meth.*, vol. A456, pp. 113-116, 2000.

[44] D. Strom, "Resistive Plate Chamber Performance in the Babar IFR System", presented at the 2001 IEEE Nuclear Science Symposium, 4-10 November, San Diego, California, USA, 2001.

[45] A. Akindinov, F. Anselmo, M. Basile, E. Cerron Zeballos, L. Cifarelli et al., "The multigap resistive plate chamber as a time-of-flight detector", *Nucl. Instr. Meth.*, vol. A456, pp. 16-22, 2000.

[46] A. Blanco, R. Ferreira-Marques, C. Finck, P. Fonte, A. Gobbi, A. Policarpo and M. Rozas, "A Large Area Timing RPC", *Nucl. Instr. Meth.* A, accepted for publication. Also preprint LIP/01-04 [Online]. Available: http://xxx. lanl. gov/abs/physics/0103086.

[47] A. Akindinov, P. Fonte, F. Formenti, V. Golovin, W. Klempt, A. Kluge et al., "A four-gap glass-RPC time of flight array with 90 ps time resolution", *IEEE Trans. Nucl. Sci.*, vol. 48, nº.5, pp.1658-1663, 2001.

[48] M. Spegel and the ALICE Collaboration, "Recent progress on RPCs for the ALICE TOF system", *Nucl. Instr. Meth.*, vol. A453, pp. 308, 2000.

[49] A. Blanco, R. Ferreira Marques, Ch. Finck, P. Fonte, A. Gobbi, S. K. Mendiratta, J. Monteiro, A. Policarpo and M. Rozas, "Development of large area and of position sensitive timing RPCs", *Nucl. Instr. Meth.*, vol. A478, pp.170-175, 2002.

[50] A. Blanco, R. Ferreira Marques, Ch. Finck, P. Fonte, A. Gobbi, A. Policarpo, "Single-Gap Timing RPCs with Bidimensional Position Sensitive Readout for Very Accurate TOF systems", presented at the the RPC2001 – 6th Workshop on Resistive Plate Chambers and Related Detectors, 26-27th November 2001, Coimbra, Portugal.

[51] E. Ceron Zeballos, I. Crotty, D. Hatzifotiadou, J. Lamas Valverde, M. C. S. Williams, A. Zichichi, P. Fonte and V. Peskov, *Nucl. Instr. Meth.* A392, pp. 150-154, 1997.

[52] A. Zallo, "The BABAR RPC system", *Nucl. Instr. Meth.*, vol. A456, pp. 117-121, 2000.

[53] K. Abe, K. Abe, H. Hanada, H. Haitani, Y. Hoshi, Y. Inoue, "Glass RPC module for the BELLE Endcap K_L/μ Detector", *Scientifica Acta*, vol. 13, pp. 281-293, 1998.

[54] K. Abe, F. Handa, I. Higuchi, Y. Hoshi, N. Kawamura, Y. Mikami, et al., "Performance of glass RPC operated in streamer mode with SF_6 gas mixture", *Nucl. Instr. Meth.*, vol. A455, pp. 397-404, 2000.

[55] M. Abbrescia, A. Colaleo, G. Iaselli, M. Maggi, B. Marangelli, S. Natali et al., Effect of the linseed oil surface treatment on the performance of resistive plate chambers", *Nucl. Instr. Meth.*, vol. A394, pp. 13-15, 1997.

[56] Yu. N. Pestov, H. R. Schmidt and B. Schreiber, "Timing performance of spark counters and photon feedback", *Nucl. Instr. Meth.*, vol. A456, pp. 11-15, 2000.

[57] B. Bartoli, R. Buonomo, E. Calloni, S. Catalanotti, B. D 'Ettore Piazzoli, G. Di Sciascio and M. Iacovacci, "Study of RPC gas mixtures for the ARGO-YBJ experiment", *Nucl. Instr. Meth.*, vol. A456, pp. 35-39, 2000.

[58] V.V.Ammosov, V.A.Gapienko, V.F.Konstantinov, Yu.M.Sviridov and V.G.Zaets, "Study of avalanche mode operation of resistive plate chambers with different gas gap structures", *Nucl. Instr. Meth.*, vol. A441, pp. 348-358, 2000.

[59] M.Adinolfi, G.Carboni, R.Messi, L.Pacciani, L.Paoluzi and E.Santovetti "Performance of low-resistivity single and dual-gap RPCs for LHCb", *Nucl. Instr. Meth.*, vol. A456, pp.95-99, 2000.

[60] M.Cwiok, W. Dominik, M.Górski and J.Krolikov, "The performance of RPCs with bakelite electrodes of various resistivity under high radiation fluxes", *Nucl. Instr. Meth.*, vol. A456, pp.87-90, 2000.

[61] G.Aielli, P.Camarri, R.Cardarelli, A.Di Ciaccio, L.Di Stante, B.Liberti, A.Paoloni and R.Santonico, "Response uniformity of a large size RPC", *Nucl. Instr. Meth.*, vol. A456, pp.40-45, 2000.

[62] G.Aielli, P.Camarri, R.Cardarelli, V.Chiostri, R.De Asmundis, A.Di Ciaccio et al., "Performance of a large-size RPC equipped with the ATLAS front-end electronics at X5-GIF irradiation facility", *Nucl. Instr. Meth.*, vol. A456, pp.77-81, 2000.

[63] M.Abbrescia, S.Altieri, G.Belli, G.Bruno, A.Colaleo, I.Crotty et al., "Performance of the RPC station prototype for the CMS barrel detector", *Nucl. Instr. Meth.*, vol. A456, pp.103-108, 2000.

[64] S.H. Ahn et al., "Performance of a large forward resistive plate chamber for the CMS/LHC under high radiation environment ", *Nucl. Instr. Meth.*, vol. A 469, pp.323-330, 2001.

[65] J.Ying, Y.L.Ye, Y.Ban, H.T.Liu, Z.M. Zhu, Z.Y.Zhu, T.Chen, J.G.Ma and S.J.Qian, "Beam test results of a resistive plate chamber made of Chinese bakelites", *Nucl. Instr. Meth.*, vol. A459, pp.513-522, 2001.

[66] Y.H.Chang, D.Chen, E.S. Hafen, P.Haridas, I.A.Pless, J.Tomasi et al., "A study of meter size RPCs for large area detectors", *Nucl. Instr. Meth.*, vol. A 349, pp.47-55, 1994.

[67] Gustavino, M.D'Incecco, E. Tatananni , G.C. Trinchero, "A glass resistive plate chamber for large experiments", *Nucl. Instr. Meth.*, vol. A457, pp. 558-563, 2001.
[68] E. Cerron Zeballos, D. Hatzifotiadou, J. Lamas Valverde, E. Platner, J. Roberts, M.C.S. Williams, A. Zichichi, "Micro-streamers and the micro-gap Resistive Plate Chamber", *Nucl. Instr. Meth.*, vol. A411, pp.51-62, 1998.
[69] G. Carlino, "The RPC trigger system of L3: history and current status", *Scientifica Acta*, vol. 13, pp. 269-280, 1998.

XIII. CAPTIONS

Fig. 1. Schematic drawing of the single-gap streamer mode RPC used by the BABAR experiment [52].

Fig. 2. Schematic drawing of the double-gap RPCs used by the L3 [69] and Belle [53] experiments.

Fig. 3. Schematic drawing of the "multigap" RPC [6].

Fig. 4. Examples of hybrid (metallic+resistive electrodes) RPC constructions. a) a four-gap counter used for timing [7]. b) microRPC [9].

Fig. 5. Survey of recently published results concerning the efficiency per gap of RPCs for MIPs (see the text for calculation details) as a function of the gap width. The efficiency decreases from 85 to 95% per gap with 2 mm gaps, irrespective of the operation mode, to 45% with 0.1 mm gaps in avalanche mode. (Main figure: n [58], £ [63], u [45], ∅ [34], — [62], [61], Œ [65], ⁄ [60], l [7], ° [59], p [39], r [64]. Inset: £ [57], u [67], ∅ [36], Œ [43], ⁄ [52], ° [66], r [53])

Fig. 6. Survey of recently published results concerning the counting rate capability of standard RPCs as a function of the resistivity of the electrodes. Only measurements taken with uniform and continuous illumination were considered. Present state-of –the-art counters reach 3 kHz/cm^2 in avalanche mode and 300 Hz/cm^2 in streamer mode. Special devices reach much higher rates (Fig. 7). (Legend: n [36], u [59], ∅ [60], Œ [68], ⁄ [62], [45], ° [62], l [64], r [63], p [65])

Fig. 7 Effective gas gain as a function of the counting rate for some special RPCs: PPAC with low resistivity anode [8] (•) and microRPC (t) [35] (see also Fig. 4). The solid line indicates the intrinsic counting rate limitation of metallic counters ([40],[42]),which is reached by both devices.

Fig. 8 Survey of recently published results concerning the time resolution of RPCs for MIPs as a function of the gap width. Most standard,2 mm gap,RPCs reach a resolution between 1 and 1.5 ns σ,independently of the operation mode. Thin gap timing RPCs reach a resolution of 50 ps σ. The time resolution of the Pestov counter is also shown for comparison [56]. (Legend: u [43], l [53], p [56], large n [57], small n [67], [39], ° [46], £ [7], Œ [45], r [65], — [64], ∅ [63], ⁄ [62]; solid symbols -streamer mode, hollow symbols – avalanche mode)

Fig. 9 Principle of operation of timing RPCs. The initial current grows exponentially in time until the discriminating level is reached. The time delay is independent from the position occupied by the initial charges, being the observed timing jitter dependent on the avalanche and cluster statistics and on the current growth rate $\alpha - \eta$.

Fig. 10 a) Schematic drawing of a microRPC with a 100 μm gap, equipped with a solid X-ray converter and anodic strips placed at a pitch of 30 μm. b) results obtained under irradiation by a soft X-ray beam collimated by a 30 μm wide slit. Each histogram was obtained at successive slit positions offset by 15 μm in digital readout mode. The first and third histograms show that mostly a single strip was hit, yielding a resolution of at least 30 μm FWHM[9].

TABLE 1: REPORTED DARK COUNT RATES OF SEVERAL COUNTERS ALONG WITH OTHER DATA OF POSSIBLE INTEREST FOR ITS INTERPRETATION

XIV. FIGURES AND TABLES

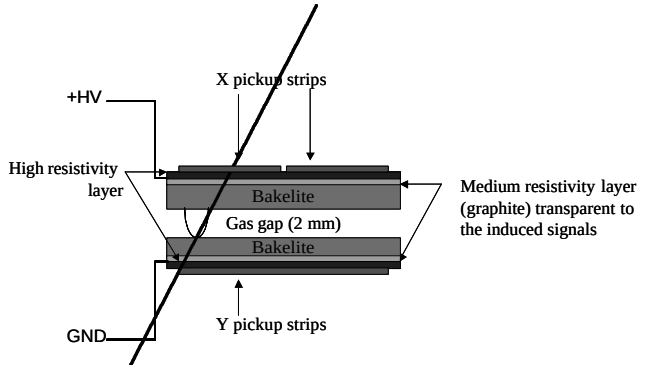

Fig. 1. Schematic drawing of the single-gap streamer mode RPC used by the BABAR experiment [52].

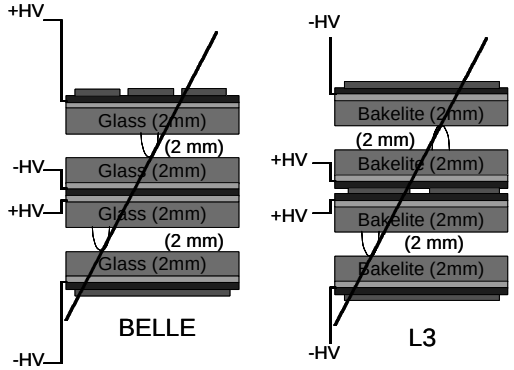

Fig. 2. Schematic drawing of the double-gap RPCs used by the L3 [69] and Belle [53] experiments.

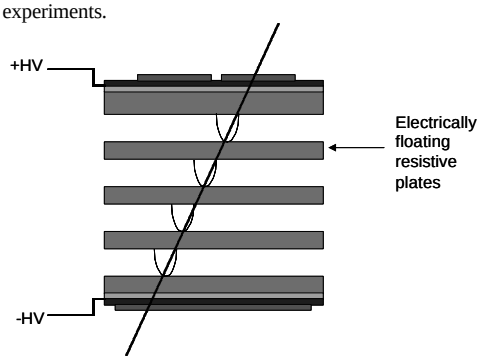

Fig. 3. Schematic drawing of the "multigap" RPC [6].

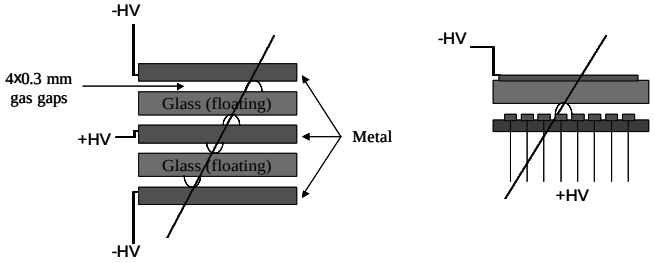

Fig. 4. Examples of hybrid (metallic+resistive electrodes) RPC constructions. a) a four-gap counter used for timing [7]. b) microRPC [9].

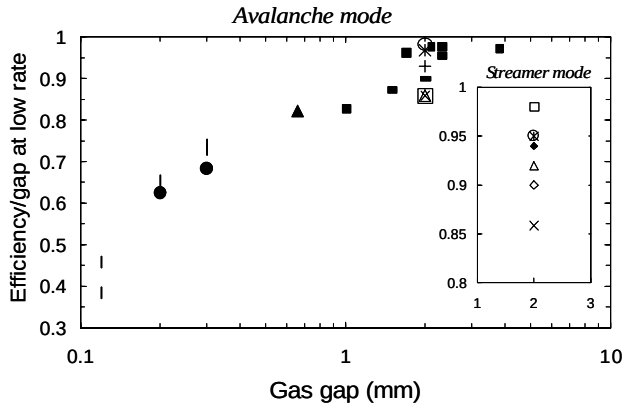

Fig. 5. Survey of recently published results concerning the efficiency per gap of RPCs for MIPs (see the text for calculation details) as a function of the gap width. The efficiency decreases from 85 to 95% per gap with 2 mm gaps, irrespective of the operation mode, to 45% with 0.1 mm gaps in avalanche mode. (Main figure: n [58], £ [63], u [45], ∅ [34], — [62], [61], Œ [65], / [60], l [7], ° [59], p [39], r [64]. Inset: £ [57], u [67], ∅ [36], Œ [43], / [52], ° [66], r [53])

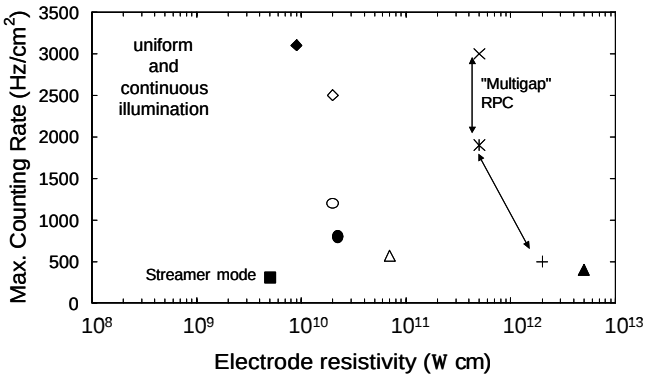

Fig. 6. Survey of recently published results concerning the counting rate capability of standard RPCs as a function of the resistivity of the electrodes. Only measurements taken with uniform and continuous illumination were considered. Present state-of –the-art counters reach 3 kHz/cm^2 in avalanche mode and 300 Hz/cm^2 in streamer mode. Special devices reach much higher rates (Fig. 7). (Legend: n [36], u [59], ∅ [60], Œ [68], / [62], [45], ° [62], l [64], r [63], p [65])

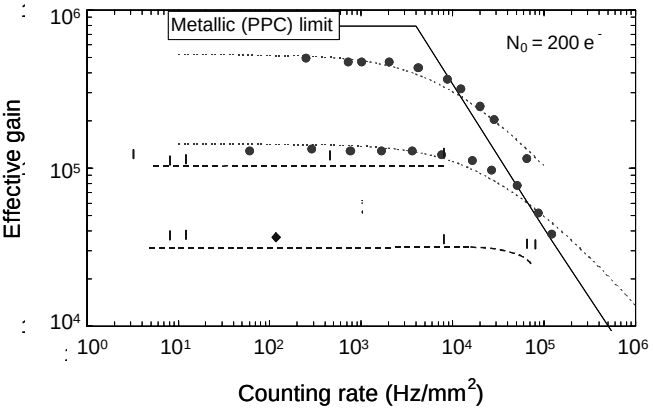

Fig. 7 Effective gas gain as a function of the counting rate for some special RPCs: PPAC with low resistivity anode [8] (●) and microRPC (t) [35] (see also Fig. 4). The solid line indicates the intrinsic counting rate limitation of metallic counters ([40],[42]),which is reached by both devices.

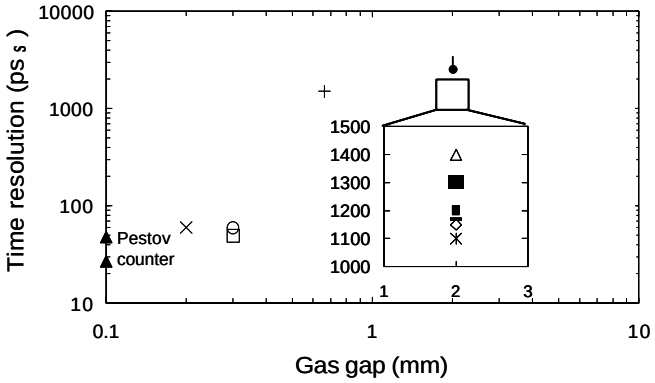

Fig. 8 Survey of recently published results concerning the time resolution of RPCs for MIPs as a function of the gap width. Most standard,2 mm gap,RPCs reach a resolution between 1 and 1.5 ns σ,independently of the operation mode. Thin gap timing RPCs reach a resolution of 50 ps σ. The time resolution of the Pestov counter is also shown for comparison [56]. (Legend: u [43], l [53], p [56], large n [57], small n [67], [39], ° [46], £ [7], Œ [45], r [65], — [64], ∅ [63], ⁄ [62]; solid symbols -streamer mode, hollow symbols – avalanche mode)

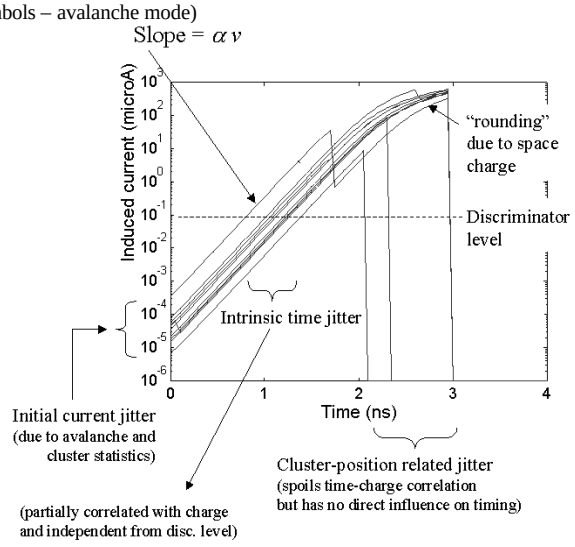

Fig. 9 Principle of operation of timing RPCs. The initial current grows exponentially in time until the discriminating level is reached. The time delay is independent from the position occupied by the initial charges, being the observed timing jitter dependent on the avalanche and cluster statistics and on the current growth $_{\text{rate}}$ α v .

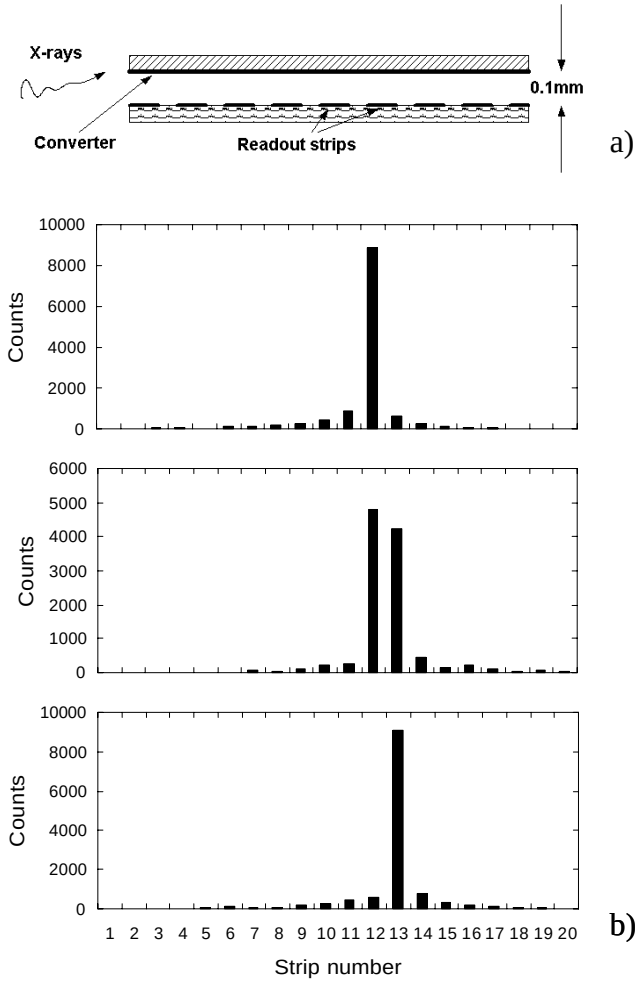

Fig. 10 a) Schematic drawing of a microRPC with a 100 μm gap, equipped with a solid X-ray converter and anodic strips placed at a pitch of 30 μm. b) results obtained under irradiation by a soft X-ray beam collimated by a 30 μm wide slit. Each histogram was obtained at successive slit positions offset by 15 μm in digital readout mode. The first and third histograms show that mostly a single strip was hit, yielding a resolution of at least 30 μm FWHM[9].

TABLE I
REPORTED DARK COUNT RATES OF SEVERAL COUNTERS ALONG WITH OTHER DATA OF POSSIBLE INTEREST FOR ITS INTERPRETATION

mode	material	gap width	rate capability (kHz/m^2)	Dark rate (kHz/m^2)	Ref.
av	glass	0.3	3000	12.5	[46]
av	melamine	0.66	19000	600	[39]
av	Si	0.4	10^8	1.6	[41]
str	bakelite	2		0.4	[57]
str	bakelite	2		1.6	[37]
str	bakelite	2	3000	0.7	[36]
str	glass	2		0.4	[53]
str	bakelite	2		1.5	[43]
str	glass	2		0.45	[54]
str	bakelite bakelite+oil	2		200 to 700 1 to 13	[55]